Thermal boundary resistance predictions from molecular dynamics simulations and theoretical calculations

E. S. Landry and A. J. H. McGaughey*
Department of Mechanical Engineering, Carnegie Mellon University, Pittsburgh, Pennsylvania 15213, USA
(Received 15 July 2009; revised manuscript received 14 September 2009; published 5 October 2009)

The accuracies of two theoretical expressions for thermal boundary resistance are assessed by comparing their predictions to independent predictions from molecular dynamics (MD) simulations. In one expression (R_E), the phonon distributions are assumed to follow the equilibrium, Bose-Einstein distribution, while in the other expression (R_{NE}), the phonons are assumed to have nonequilibrium, but bulk-like distributions. The phonon properties are obtained using lattice dynamics-based methods, which assume that the phonon interface scattering is specular and elastic. We consider (i) a symmetrically strained Si/Ge interface, and (ii) a series of interfaces between Si and "heavy-Si," which differs from Si only in mass. All of the interfaces are perfect, justifying the assumption of specular scattering. The MD-predicted Si/Ge thermal boundary resistance is temperature independent and equal to 3.1×10^{-9} m^2-K/W below a temperature of ~500 K, indicating that the phonon scattering is elastic, as required for the validity of the theoretical calculations. At higher-temperatures, the MD-predicted Si/Ge thermal boundary resistance decreases with increasing temperature, a trend we attribute to inelastic scattering. For the Si/Ge interface and the Si/heavy-Si interfaces with mass ratios greater than two, R_E is in good agreement with the corresponding MD-predicted values at temperatures where the interface scattering is elastic. When applied to a system containing no interface, R_E is erroneously nonzero due to the assumption of equilibrium phonon distributions on either side of the interface. While R_{NE} is zero for a system containing no interface, it is 40%–60% less than the corresponding MD-predicted values for the Si/Ge interface and the Si/heavy-Si interfaces at temperatures where the interface scattering is elastic. This inaccuracy is attributed to the assumption of bulk-like phonon distributions on either side of the interface.

DOI: 10.1103/PhysRevB.80.165304 PACS number(s): 67.30.hp, 44.10.+i, 63.22.−m, 65.40.−b

I. INTRODUCTION

A. Background

The scattering of thermal energy carriers (i.e., electrons and phonons) at an interface between two solids results in a thermal boundary resistance.[1] An ability to accurately predict thermal boundary resistance (or its inverse, the thermal boundary conductance) is valuable in the thermal analysis of devices where the average distance between nonmetal/nonmetal or metal/nonmetal interfaces is on the same scale as the carrier mean free paths. For example, the distance between interfaces in the active region in semiconductor lasers and light-emitting diodes is 1–10 nm.[2,3] The ability to predict thermal boundary resistance will also lead to improvements in the design of semiconductor superlattices (periodic nanostructures containing many interfaces) with low-thermal conductivity for thermoelectric energy conversion applications.[4,5]

The most commonly applied theoretical models for predicting thermal boundary resistance are the acoustic mismatch model (AMM) and the diffuse mismatch model (DMM).[1,6] At temperatures less than ~30 K, the AMM and DMM predict similar values for the thermal boundary resistance that are in reasonable agreement with experimental measurements.[1] At typical application temperatures, however, assumptions in the AMM and DMM make their predictions inaccurate. Both models assume that the thermal transport is dominated by phonons, which is valid for interfaces between dielectrics or lightly doped semiconductors. There are differing views, however, on the role of electron-phonon coupling at metal/dielectric interfaces,[7–9] to which all of the experimental data correspond due to metrological limitations. In the DMM, the phonon interface scattering is assumed to be diffuse (i.e., the incident phonon loses all memory of its direction and polarization) while the AMM assumes that there is no probability of diffuse scattering (i.e., specular scattering). The actual degree of specular and diffuse scattering is dependent on the interface quality,[1,10,11] which is often known only qualitatively. In addition, both models neglect the atomic-level detail of the interface and are usually applied under the Debye approximation of linear phonon dispersion curves.[12–18] These two assumptions lead to inaccuracy at temperatures where phonons with wavelengths on the same scale as the interatomic spacing are excited.[19] Furthermore, both the AMM and DMM assume that the phonon interface scattering is elastic (i.e., the reflected and transmitted phonons have the same frequency as the incident phonon). This assumption leads to a prediction of (i) a constant thermal boundary resistance in the classical limit, reached when all of the phonon modes are fully excited, and (ii) a lower bound on the thermal boundary resistance known as the phonon radiation limit.[1,7,20,21] Contrary to these predictions, a thermal boundary resistance that decreases with increasing temperature in the classical limit,[9,14,15] and values below the phonon radiation limit,[7,9,21] have been experimentally measured. These results have been attributed to the presence of inelastic phonon scattering at the interface.

One approach for developing improved models for thermal boundary resistance is to modify the AMM or DMM to include phenomena neglected in the original models (e.g., phonon scattering near the interface,[16] interface disorder,[12,13]

 ©2009 The American Physical Society

and electron-phonon coupling[8]). While the predictions of the modified models are generally in better agreement with experiment than the original AMM or DMM, they have only been applied under the Debye approximation and in some cases require fitting parameters.[16] The enhanced agreement with experiment may therefore be fortuitous. In our opinion, the correct way to develop improved models is to use atomic-level methods to better understand the phonon transport physics. In this way, models can be developed based on justifiable assumptions.

B. Atomic-level methods

Molecular dynamics (MD) simulation is an atomic-level method that has been used to model thermal transport across interfaces[22–27] and in superlattices.[28–32] In an MD simulation, the positions and momenta of a set of atoms evolve classically according to Newtonian equations of motion, restricting their validity to the classical limit. In this limit, MD simulation is an ideal method for predicting thermal boundary resistance because no assumptions concerning the nature of the phonon scattering are required. The only required input to an MD simulation is a method for specifying the atomic interactions. Because simulation cells containing 10^4-10^5 atoms are required to remove the thermal boundary resistance dependence on cell-size, the use of *ab initio* [e.g., density functional theory (DFT)]-based methods is precluded due to computational expense. The specification of the atomic interactions is thus typically done using empirical interatomic potential functions. Beyond obtaining a prediction for the thermal boundary resistance, it is challenging to extract additional details related to the thermal transport physics from an MD simulation due to computational expense.[33–35]

The details of the thermal transport physics can be studied using lattice dynamics[36–38] (LD) or nonequilibrium Green's function[39] (NEGF)-based methods. Using the phonon properties calculated from these methods, the thermal boundary resistance can be predicted by evaluating a theoretical expression, such as that derived using theory analogous to the Landauer theory for electron transport.[40] The LD and NEGF-based methods can be used to obtain phonon properties at temperatures where quantum effects are important (i.e., below the Debye temperature).[40] The effects of inelastic scattering can be modeled using the NEGF-based approach, though such calculations have only been performed for one-dimensional systems due to computational expense.[38,40,41] To reduce the computational expense when modeling interfaces, the harmonic approximation is typically applied, removing all crystal anharmonicity and thus limiting the calculation accuracy to interfaces at which the phonon scattering is elastic.[36–39] As with MD simulation, the LD- and NEGF-based methods require a method to specify the atomic interactions. Because only the second-order force constants are required under the harmonic approximation, either empirical interatomic potential functions or *ab initio*-based methods can be used. To our knowledge, only empirical interatomic potential functions have been used to date.

C. Objectives

Despite over five decades of research, a robust model for the thermal boundary resistance has remained elusive.[1,6] In our view, the development of such a model has been slowed by the many sources of uncertainty when comparing theoretical predictions and experimental measurements (e.g., the roles of electron-phonon coupling, interface quality, and inelastic phonon scattering). The objective of this work is to assess the theory for thermal transport by phonons across an interface by eliminating these sources of uncertainty. We achieve this objective by evaluating theoretical expressions for the thermal boundary resistance using phonon properties obtained from LD-based calculations and comparing the results to independent MD-predicted values in a self-consistent manner. In both the theoretical and MD predictions, there is no electronic contribution to the thermal transport and we study perfect interfaces between two crystals that contain no defects. The theoretical expressions are evaluated in the classical limit, as required for the validity of the MD simulations. In addition, the comparison is performed at temperatures where we demonstrate that the phonon interface scattering is elastic, as required for the validity of the LD-based calculations.

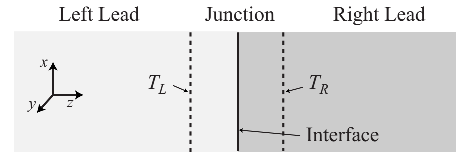

FIG. 1. Schematic diagram of an interface between two semi-infinite leads. Under the assumption of no inelastic scattering within the junction, the thermal boundary resistance is equal to the junction thermal resistance.

We consider two types of interface: (i) a symmetrically-strained Si/Ge interface, and (ii) a series of interfaces between Si and a species we refer to as "heavy-Si," which differs from Si only in mass by a ratio of m_R. For the Si/heavy-Si interfaces, we consider mass ratios between 1 and 6. For comparison, the mass ratio between Ge and Si is 2.6. Each interface is oriented along the (001) crystallographic plane (see coordinate system in Fig. 1). The atomic interactions are modeled using the Stillinger-Weber (SW) interatomic potential, which has been parameterized for both Si-Si and Ge-Ge interactions.[42,43] For the Si-Ge interactions, we use the mixing rules described by Laradji *et al.*[44] The details related to the theoretical calculations and MD simulations are described in Secs. II C and III, and the results of the comparison are provided in Sec. IV.

II. THERMAL TRANSPORT ACROSS AN INTERFACE

A. Overview

We begin by reviewing the theory for thermal transport by phonons across an interface. To increase the generality of the discussion, we describe this theory for a system containing a junction between two semi-infinite solids (i.e., leads), as shown in Fig. 1 for our case, where the junction contains the interface. This theory has been applied to predict the thermal resistance of a variety of junction types, including dielectric quantum wires,[45] carbon nanotubes,[46] grain boundaries,[23,24] and interfaces.[19,36–38,47,48]

We will develop two expressions for the junction thermal resistance, R, defined as

$$R = \frac{T_L - T_R}{q}, \tag{1}$$

where q is the heat flux across the junction, and T_L and T_R are the temperatures at the lead/junction boundaries. When we evaluate these expressions (discussed in Sec. II C), we will assume that there is no inelastic scattering within the junction. Under this assumption, the thermal boundary resistance, which is defined in terms of the temperature drop across the interface, is equal to the junction thermal resistance, regardless of the junction width.

Each lead emits phonons to and absorbs phonons from the junction. At steady-state, the net heat flux across the junction is

$$q = \frac{1}{(2\pi)^3}\int_L \sum_{\nu}^{+} \hbar\omega(\boldsymbol{\kappa},\nu)v_z(\boldsymbol{\kappa},\nu)\alpha_{L\to R}(\boldsymbol{\kappa},\nu)f_L(\boldsymbol{\kappa},\nu)d\boldsymbol{\kappa} + \frac{1}{(2\pi)^3}\int_R \sum_{\nu}^{-} \hbar\omega(\boldsymbol{\kappa},\nu)v_z(\boldsymbol{\kappa},\nu)\alpha_{R\to L}(\boldsymbol{\kappa},\nu)f_R(\boldsymbol{\kappa},\nu)d\boldsymbol{\kappa}, \tag{2}$$

where L and R denote the left and right leads, $\hbar$ is the Planck constant divided by 2π, ν denotes the phonon polarization, and $\boldsymbol{\kappa}$, ω, and v_z are the phonon wave-vector, frequency, and z component of the group velocity. The first (second) integral is over the first Brillouin zone of the left (right) lead, and the first (second) summation is over phonons moving in the positive (negative) z-direction. The mode-dependent phonon transmission coefficient, $\alpha_{L\to R}$, is defined as the fraction of the incident phonon energy that is transmitted from the left lead to the right lead (similar for $\alpha_{R\to L}$). The variables f_L and f_R are the mode-dependent phonon distributions functions in the left and right leads at the lead/junction boundaries. We write these distributions as

$$f_L(\boldsymbol{\kappa},\nu) = f_{\mathrm{BE}}[\omega(\boldsymbol{\kappa},\nu),T_L] + f_L'(\boldsymbol{\kappa},\nu)$$

$$f_R(\boldsymbol{\kappa},\nu) = f_{\mathrm{BE}}[\omega(\boldsymbol{\kappa},\nu),T_R] + f_R'(\boldsymbol{\kappa},\nu), \tag{3}$$

where f_{BE} is the equilibrium Bose-Einstein distribution function, and f_L' and f_R' are the deviations from the equilibrium distribution. The equilibrium distribution is

$$f_{\mathrm{BE}}(\omega,T) = \left[\exp\left(\frac{\hbar\omega}{k_{\mathrm{B}}T}\right) - 1\right]^{-1}, \tag{4}$$

where k_{B} is the Boltzmann constant. We define the temperature of a nonequilibrium system to be that of an equilibrium system with the same kinetic energy.[11,47] The temperatures at the lead/junction boundaries are therefore equal to T_L and T_R if

$$\frac{1}{(2\pi)^3}\int \sum_{\nu} \hbar\omega f' d\boldsymbol{\kappa} = 0 \tag{5}$$

in each lead.

B. Junction thermal resistance

1. R_E

The first expression we derive for the junction thermal resistance is analogous to the Landauer formula for electron transport,[40] and is based on the assumption that each lead is an infinite thermal reservoir held in equilibrium at a uniform temperature. Under this assumption, $f_L' = f_R' = 0$ for all modes, and Eq. (2) becomes

$$q = \frac{1}{(2\pi)^3}\int_L \sum_{\nu}^{+} \hbar\omega v_z \alpha_{L\to R} f_{\mathrm{BE}}(\omega,T_L)d\boldsymbol{\kappa} + \frac{1}{(2\pi)^3}\int_R \sum_{\nu}^{-} \hbar\omega v_z \alpha_{R\to L} f_{\mathrm{BE}}(\omega,T_R)d\boldsymbol{\kappa}. \tag{6}$$

When $T_L = T_R$, the two terms on the right hand side of Eq. (6) must cancel to give zero heat flux at thermal equilibrium. This condition allows Eq. (6) to be simplified to involve integration over just one of the leads. For example, if both leads are at a temperature of T_R,

$$\frac{1}{(2\pi)^3}\int_R \sum_{\nu}^{-} \hbar\omega v_z \alpha_{R\to L} f_{\mathrm{BE}}(\omega,T_R)d\boldsymbol{\kappa} = -\frac{1}{(2\pi)^3}\int_L \sum_{\nu}^{+} \hbar\omega v_z \alpha_{L\to R} f_{\mathrm{BE}}(\omega,T_R)d\boldsymbol{\kappa}, \tag{7}$$

allowing Eq. (6) to be simplified to

$$q = \frac{1}{(2\pi)^3}\int_L \sum_{\nu}^{+} \hbar\omega v_z \alpha_{L\to R}[f_{\mathrm{BE}}(\omega,T_L) - f_{\mathrm{BE}}(\omega,T_R)]d\boldsymbol{\kappa}. \tag{8}$$

In writing Eq. (8), we have assumed that the phonon properties are temperature independent between temperatures of T_L and T_R. After substituting Eq. (8) into Eq. (1), and expanding $f_{\mathrm{BE}}(\omega,T_L) - f_{\mathrm{BE}}(\omega,T_R)$ using a first-order Taylor series, the thermal resistance is found to be

$$R_E = \left[\frac{1}{(2\pi)^3}\int_L \sum_{\nu}^{+} \hbar\omega v_z \alpha_{L\to R}\frac{df_{\mathrm{BE}}}{dT}d\boldsymbol{\kappa}\right]^{-1}, \tag{9}$$

where the subscript E denotes that the phonons in the leads follow the equilibrium distribution function, Eq. (4).

Due to its simplicity, Eq. (9) is the most commonly applied expression for calculating thermal resistance.[19,23,24,36–38,47,48] It is well known, however, that this expression is inaccurate when the average phonon transmission coefficient approaches unity.[1,49] For example, when Eq. (9) is applied to a perfect crystal (i.e., a system containing no interface), $\alpha_{L\to R} = 1$ for all phonon modes, and the incorrect result of a nonzero thermal resistance is predicted. The theory underlying Eq. (9) also contains an inconsistency, as it suggests that at steady state, there is simultaneously zero heat flux within the leads (where there is no temperature gradient) and a nonzero heat flux across the junction.[6,49] This

inconsistency and the erroneous prediction for the no-interface case both result from the assumption that f'_L and f'_R are equal to zero.[49]

2. R_{NE}

Following the approach of Simons,[49] we now derive an expression for the junction thermal resistance that is valid for nonequilibrium phonon distributions in each lead, which we denote by R_{NE}. Our expression is more general than that given by Simons because we do not make the Debye approximation for the phonon dispersion. The thermal resistance is found by substituting Eq. (2) into Eq. (1) [using the general forms for f_L and f_R given in Eq. (3)], and simplifying using a procedure similar to that described in the development of Eq. (9). The resulting expression is

$$R_{NE} = \gamma R_E, \tag{10}$$

where

$$\gamma = 1 - \frac{1}{(2\pi)^3}\int_L \sum_{\nu}^{+} \beta_L \alpha_{L\to R} d\boldsymbol{\kappa} - \frac{1}{(2\pi)^3}\int_R \sum_{\nu}^{-} \beta_R \alpha_{R\to L} d\boldsymbol{\kappa}, \tag{11}$$

and β is the fraction of the total heat flux carried by a specific phonon mode in the lead, given by

$$\beta = \frac{\hbar\omega v_z f'}{q}. \tag{12}$$

For the case where no interface is present, $\alpha_{L\to R}=1$ for all phonon modes and both terms involving integrals in Eq. (11) are equal to 1/2, leading to the correct result of zero thermal resistance.

To evaluate R_{NE} for a general system, we need to specify the mode-dependent deviations from the equilibrium phonon distributions, f', that appear in Eq. (12). This specification can be done by solving the Boltzmann transport equation (BTE), which describes the spatial and temporal variation of the distribution of a collection of particles subject to an applied field (e.g., electrons subject to an electric field, phonons subject to a temperature gradient).[11] Exact solution of the BTE is challenging for the lead/junction/lead system because the phonon distributions in the leads are coupled due to energy transmission across the junction. To simplify the solution procedure, we follow the approach of Chen[50] by assuming that the phonon distribution in each lead near the junction is bulk-like, allowing the BTE to be solved independently for each lead. We will discuss the accuracy of this assumption in Sec. IV.

For a system of phonons subject to a temperature gradient in one-dimension, the steady-state BTE for a specific phonon mode takes the form[11]

$$v_z \frac{\partial f}{\partial z} = \left(\frac{\partial f}{\partial t}\right)_{\text{coll}}, \tag{13}$$

where $(\partial f/\partial t)_{\text{coll}}$ is the collision term, which describes the rate of change of the phonon distribution due to phonon scattering. We apply the relaxation time approximation by writing the collision term as

$$\left(\frac{\partial f}{\partial t}\right)_{\text{coll}} = -\frac{f'}{\tau}, \tag{14}$$

where τ is the phonon relaxation time, and assume f' to be independent of temperature so that

$$\frac{\partial f}{\partial z} = \frac{\partial f_{\text{BE}}}{\partial T}\frac{\partial T}{\partial z}. \tag{15}$$

After substituting Eqs. (14) and (15) into Eq. (13), f' is found to be

$$f' = -v_z \tau \frac{\partial f_{\text{BE}}}{\partial T}\frac{\partial T}{\partial z}. \tag{16}$$

Using this result and the Fourier law, $q=-k\frac{\partial T}{\partial z}$, we can rewrite Eq. (12) as

$$\beta = \frac{\hbar\omega v_z^2 \tau}{k}\frac{\partial f_{\text{BE}}}{\partial T}, \tag{17}$$

where the thermal conductivity, k, is given by

$$k = \frac{1}{(2\pi)^3}\int \sum_{\nu} \hbar\omega v_z^2 \tau \frac{df_{\text{BE}}}{dT} d\boldsymbol{\kappa}. \tag{18}$$

When f' is specified using the approach described in this section and the lead species are identical, Eq. (10) can be reduced to the inverse of the formula provided by Aubry *et al.*[24] for the thermal conductance of a grain boundary. In arriving at their expression, Aubry *et al.* take the temperature associated with an incident phonon to be the local temperature at a distance of $v_z\tau$ (i.e., one mean-free path) from the grain boundary instead of T_L or T_R. We believe that our development, which mirrors that of Simons,[49] has two advantages over this approach. First, the assumptions made in arriving at Eq. (16) for f' are easily identified, allowing an avenue for further investigation into sources of inaccuracy. Second, this approach can be used to specify f' for phonons moving away from the junction, allowing for a consistent definition for T_L and T_R to be maintained [see discussion preceding Eq. (5)].

C. Lattice dynamics-based calculations of R_E and R_{NE}

1. Phonon properties

We evaluate R_E and R_{NE} for the Si/Ge and Si/heavy-Si interfaces using Monte Carlo integration with 10^5 random phonon wave vectors in the first Brillouin zone corresponding to the two-atom diamond unit cell. For comparison to the classical MD-based predictions (discussed in Sec. III), these calculations are performed in the classical limit by setting $f_{\text{BE}}=k_{\text{B}}T/\hbar\omega$. At each wave vector, the frequencies and group velocities are obtained using LD-calculations applied under the harmonic approximation. Under this approximation, the atomic interactions are modeled by expanding the crystal potential energy about its minimum using a Taylor series and truncating after the second-order term. For stiff materials with small thermal expansion coefficients such as SW Si and Ge, this approximation yields accurate predictions for phonon frequencies and group velocities (e.g., pho-

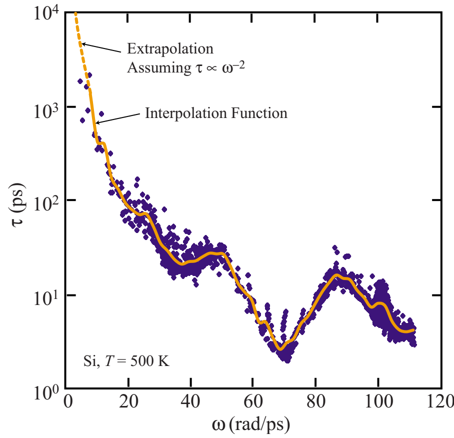

FIG. 2. (Color online) Classical phonon relaxation times in the first Brillouin zone for SW Si predicted using anharmonic LD-based calculations at a temperature of 500 K.

non frequencies calculated using harmonic and anharmonic LD-based methods differ by less than 3% in SW Si below temperatures of 1000 K[51]). The phonon transmission coefficients are obtained using the harmonic LD-based scattering boundary method,[38,40,52] which assumes that the phonon interface scattering is specular and elastic. We believe that the assumption of specular scattering is valid for our interfaces because they contain no defects or roughness that would promote diffuse scattering.[1,11] In Sec. IV A, we demonstrate that the phonons scatter elastically at our interfaces at temperatures less than or equal to ~500 K. Full details related to our harmonic LD-based calculations can be found elsewhere.[27,53,54]

The phonon relaxation times are calculated using an anharmonic LD-based method that approximates the crystal anharmonicity by treating the third- and fourth-order terms in the Taylor series expansion of the potential energy as a perturbation to the harmonic solution.[51] For all phonon modes, we find that the calculated relaxation time is proportional to T^{-1} to within 5% accuracy between temperatures of 300 and 1000 K. In addition, at a fixed temperature, the relaxation times can be approximated as a function of frequency alone, as shown in Fig. 2 for SW Si at a temperature of 500 K. Based on these observations, we generate a linear interpolation function using the GNU Scientific Library[64] for each species based on the calculated relaxation times at a temperature of 500 K. These interpolation functions are used with the T^{-1} proportionality to specify the relaxation time for any phonon mode and temperature. At low frequencies, we extrapolate the calculated relaxation times by assuming that $\tau \propto \omega^{-2}$, as predicted by Callaway.[55] At high temperatures, fifth- and higher-order terms in the Taylor series expansion may not be negligible, leading to a potential source of inaccuracy in the calculated relaxation times.[56] While it is difficult to quantify this inaccuracy, we expect that its effect on our R_{NE} calculations will be partially abated due to error cancellation resulting from the relaxation times appearing in both the numerator and denominator (through the thermal conductivity) of Eq. (17).

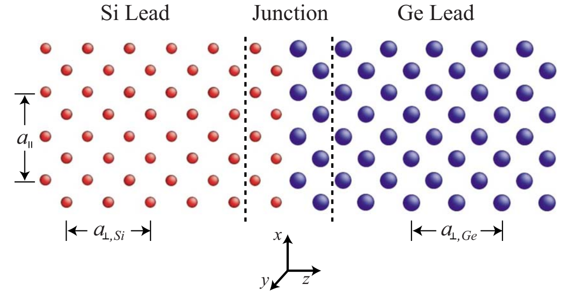

FIG. 3. (Color online) Schematic diagram of the symmetrically strained Si/Ge interface.

2. Interface structure

A schematic diagram of the symmetrically-strained Si/Ge interface modeled in our LD-based calculations is shown in Fig. 3. Only a portion of the interface is shown, as the leads are assumed to be semi-infinite in the calculations. The atomic positions are set using a lattice constant in the directions parallel to the interface, $a_{\parallel}$, equal to the average of the bulk zero stress, zero-temperature SW Si and Ge lattice constants, a_{Si} and a_{Ge} of 5.430 95 Å and 5.653 62 Å. The lead lattice constants in the direction perpendicular to the interface, $a_{\perp}$, are chosen to give zero stress in that direction and are determined by minimizing the lead potential energy while keeping the parallel lattice constant fixed at $a_{\parallel}$. These lattice constants are 5.318 30 Å and 5.735 27 Å for SW Si and Ge. The distances between the monolayers within the junction are determined by relaxing the structure using a steepest decent approach. In our calculations, the junction contains the two monolayers on either side of the interface. We find that increasing the size of the junction in the z direction has no effect on the calculated value of the thermal boundary resistance. For the Si/heavy-Si supercells, there is no lattice mismatch between the species and the atomic positions are set using a_{Si}.

III. MOLECULAR DYNAMICS SIMULATIONS

A. Direct method

To assess the accuracy of the theoretical expressions for the thermal boundary resistance, we compare their predictions to independent predictions obtained from MD simulations, which as described in Sec. I B, require no assumptions about the nature of the phonon scattering. In our MD simulations, the Newtonian equations of motion are integrated numerically using the velocity Verlet algorithm with a time step of 0.55 fs. We predict the thermal boundary resistance using the direct method, in which a known heat flux is applied across the sample and the resulting steady-state temperature drop at the interface is specified. The thermal boundary resistance is then determined from Eq. (1). A schematic diagram of the direct method simulation cell is shown in Fig. 4. The system consists of a sample region containing two materials of lengths L_L and L_R in contact, forming a single interface. The sample region is bordered by hot and cold reservoirs of length L_{res} and fixed boundaries in the z direction. The fixed boundary regions each contain four

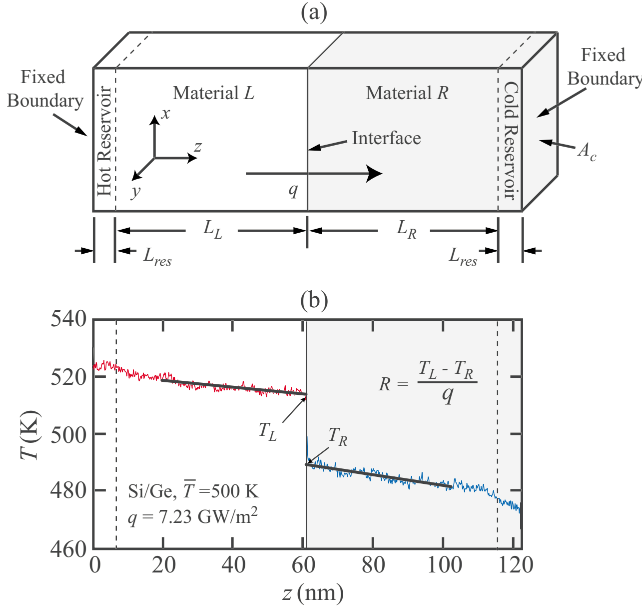

FIG. 4. (Color online) (a) Direct method simulation cell. (b) Temperature profile for the symmetrically strained Si/Ge interface at a temperature of 500 K using the simulation parameters provided for case A in Table I.

monolayers of fixed atoms in order to prevent reservoir atoms from sublimating. The cross-section of the simulation cell is square and has area A_c. Periodic boundary conditions are imposed in the x and y directions.

B. Structure

The initial atomic positions are chosen to obtain relaxed structures in a manner similar to that used for the LD-based calculations (described in Sec. II C 2). In our MD simulations, however, we also account for the temperature dependence of the bulk lattice constants, though we find that it has negligible effect on the predicted thermal boundary resistance. From separate MD simulations run at constant temperature and zero pressure using a Nose-Hoover thermostat and a Berendsen barostat, we find that the bulk lattice constants of SW Si and Ge are approximated to within 0.02% between temperatures of 300 and 1000 K by

$$a_{\mathrm{Si}}(T) = 5.430 + 1.975 \times 10^{-5}T \ [\text{Å}] \qquad (19)$$

$$a_{\mathrm{Ge}}(T) = 5.654 + 3.205 \times 10^{-5}T \ [\text{Å}], \qquad (20)$$

where T is in Kelvin. When assigning the initial atomic positions for the direct method simulations, we evaluate the bulk lattice constants using the average temperature in the simulation cell, $\bar{T}$. The z components of the initial atomic positions are set using species-dependent perpendicular lattice constants that lead to zero stress in the z direction. These perpendicular lattice constants are calculated from elasticity theory to be[57]

$$a_{\perp} = a\left[1 - \frac{2C_{12}}{C_{11}}\left(\frac{a_{\parallel}}{a} - 1\right)\right], \qquad (21)$$

where C_{11} and C_{12} are the elastic constants. Using the analytical method described by Cowley,[58] we calculate C_{11} and C_{12} to be 151.6 and 76.5 GPa for SW Si, and 138.3 and 50.9 GPa for SW Ge.

C. Data collection and analysis

In the direct method simulations, the sample and reservoirs are initially set to a uniform temperature by scaling the atomic velocities for 0.55 ns (one million time steps), a period in which the structure also experiences a slight relaxation. The heat flux is then applied by adding a constant amount of kinetic energy to the hot reservoir and removing the same amount of kinetic energy from the cold reservoir at every time step using the method described by Ikeshoji and Hafskjold.[59] From this point, a period of 3.3 ns is allowed for the sample to reach steady-state conditions. Data are collected for an additional 2.75 ns after this period for the thermal boundary resistance prediction.

The steady-state temperature profile is obtained by averaging the temperature of each monolayer over the data collection period. An example temperature profile is shown in Fig. 4(b) for the symmetrically strained Si/Ge interface at a temperature of 500 K. To minimize the uncertainty in specifying the temperature drop at the interface, we apply a least-squares linear regression analysis to the temperature profile in each material and evaluate the linear fits at the interface. The nonlinear regions in the temperature profile found in the 100 monolayers closest to the reservoir/sample boundary are neglected when performing the regression analysis, as shown in Fig. 4(b). We estimate the uncertainty in specifying the temperature drop at the interface to be ±5% based on the sensitivity of the linear fits to the number of monolayers used in the regression analysis.

D. Effect of the simulation parameters on the thermal boundary resistance

The primary challenge associated with the direct method is to obtain thermal boundary resistance predictions that are independent of the simulation parameters, q, L_L, L_R, L_{res}, and A_c, and the sample orientation (i.e., the sample can be oriented with either species on the hot side of the simulation cell). For example, when L_L or L_R is not much greater than the bulk phonon mean free path, phonons can travel ballistically from the reservoirs to the interface. In addition, if the value of the heat flux is too large, nonlinear temperature profiles may develop throughout the sample due to the temperature dependence of the thermal conductivity. Both of these effects lead to unrealistic incident phonon distributions and may influence the predicted value of the thermal boundary resistance.

In Table I, the effects of the simulation parameters on the predicted thermal boundary resistance of the Si/Ge interface at a temperature of 500 K are shown. The thermal boundary resistance provided for case A is the 95% confidence interval based on the results of five independent simulations while for

TABLE I. Effect of the direct method simulation parameters (q, L_L, L_R, L_{res}, A_c, and sample orientation) on the MD-predicted thermal boundary resistance of the Si/Ge interface at a temperature of 500 K. For the sample orientation, Si/Ge (Ge/Si) indicates that Si (Ge) is on the hot side and Ge (Si) is on the cold side of the simulation cell. The thermal boundary resistance provided for case A is the 95% confidence interval based on the results of five independent simulations.

	q (GW/m^2)	$L_L=L_R$ (monolayers)	L_{res} (monolayers)	$A_c/a_\parallel^2$	Orientation	R (10^{-9} m^2 K/W)
A	7.23	400	50	16	Si/Ge	2.93 ± 0.29 (95%)
B	7.23	400	50	16	Ge/Si	2.94
C	3.10	400	50	16	Si/Ge	3.02
D	13.4	400	50	16	Si/Ge	2.97
E	7.23	200	50	16	Si/Ge	4.01
F	7.23	300	50	16	Si/Ge	3.22
G	7.23	500	50	16	Si/Ge	2.72
H	7.23	600	50	16	Si/Ge	2.83
I	7.23	400	20	16	Si/Ge	3.17
J	7.23	400	100	16	Si/Ge	2.95
K	7.23	400	50	25	Si/Ge	3.13
L	7.23	400	50	36	Si/Ge	2.81

the other cases, the provided value is the result of one simulation. The thermal boundary resistance is independent of the imposed heat flux (compare cases A, C, and D), reservoir length (cases A, I, and J), and cross-sectional area (cases A, K, and L) over the range of values considered. The thermal boundary resistance is found to decrease with increasing L_L and L_R until size-independent results are obtained when L_L and L_R are greater than or equal to 400 monolayers (cases A and E-H). The thermal boundary resistance is also independent of the sample orientation, see cases A and B.

Based on the results presented in Table I, we believe that the thermal boundary resistance predicted for the Si/Ge interface at a temperature of 500 K is independent of the simulation parameters when using the parameters provided for case A. We use these parameters for all of our direct method simulations at temperatures greater than or equal to 500 K. At temperatures lower than 500 K, however, these parameters may not be sufficient to remove the simulation cell size effects. To ensure that these effects are negligible, we use simulation cells with $L_L=L_R=700$ monolayers and $L_L=L_R=500$ monolayers at temperatures of 300 K and 400 K. These values of L_L and L_R are roughly a factor of $500/T$ greater than the values provided for case A. This factor is chosen based on the fact that thermal conductivity of a crystal is approximately proportional to T^{-1} in the classical limit (reached in the MD system), and on the kinetic theory prediction that the average phonon mean free path is proportional to the thermal conductivity.[60]

IV. RESULTS

A. Molecular dynamics predictions

The MD predictions of the thermal boundary resistance for the symmetrically strained Si/Ge interface between temperatures of 300 K and 1000 K are shown in Fig. 5. Error bars representing the 95% confidence interval based on five independent simulations are provided for each data point. We observe a low-temperature regime, in which the thermal boundary resistance is temperature independent and equal to $\sim 3.1 \times 10^{-9}$ m^2-K/W, and a high-temperature regime in which the thermal boundary resistance decreases with increasing temperature. The boundary between these regimes exists at a temperature between 400 and 500 K.

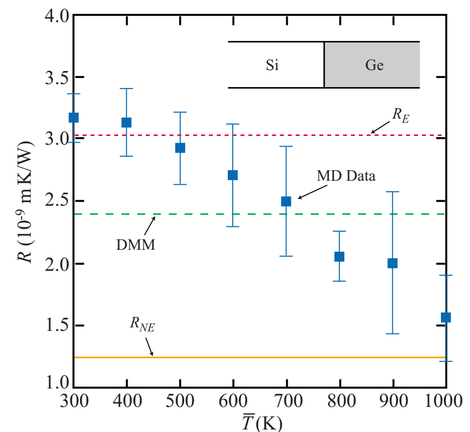

FIG. 5. (Color online) Temperature dependence of the thermal boundary resistance of a symmetrically strained Si/Ge interface. The error bars provided for the MD-predicted values represent the 95% confidence interval based on five independent simulations. The lines labeled R_E and R_{NE} correspond to the results of theoretical calculations assuming that the phonons scatter elastically and specularly at the interface and have either equilibrium or bulk-like nonequilibrium distributions (see Sec. II B). The line labeled DMM corresponds to the theoretical calculation of the diffuse mismatch model, which assumes that the phonons scatter elastically and diffusely at the interface and have equilibrium distributions.

As mentioned in Sec. I, experimental measurements of the thermal boundary resistance of an isolated interface have only been made for metal/dielectric interfaces. To provide a comparison to our MD predictions, we estimate the experimental Si/Ge thermal boundary resistance based on the thermal conductivity measurements of Borca-Tasciuc *et al.* for undoped, symmetrically strained Si/Ge superlattices.[61] For a Si/Ge superlattice with interfaces separated by 7 nm, they measured the thermal conductivity in the direction perpendicular to the interfaces to be 2.9 W/m-K at a temperature of 300 K.[61] By assuming that the dominant source of thermal resistance in these superlattices is due to the interfaces, we estimate the experimental Si/Ge thermal boundary resistance to be of order 10^{-9} m^2-K/W,[62] in agreement with our MD-predicted values.

We attribute the MD-predicted temperature dependence of the Si/Ge thermal boundary resistance at high temperatures to inelastic phonon interface scattering, which (i) increases with increasing temperature due to increasing anharmonicity of the atomic interactions, and (ii) tends to increase the phonon transmission coefficients.[1] We believe that this mechanism dominates over other potential mechanisms, which we identify from the theoretical expressions for thermal boundary resistance (see Sec. II B). First, the temperature dependence of the phonon frequencies and group velocities is negligible for SW Si and Ge, and $\partial f_{\mathrm{BE}}/\partial T$ is a constant in the classical limit (see Sec. II C 1). Second, the temperature-dependence of the lead thermal conductivities is canceled by the temperature dependence of the phonon relaxation times in Eq. (17). We therefore take the temperature independence of the thermal boundary resistance in the low-temperature regime as an indication that the phonon interface scattering there is elastic.

An intuitive explanation for why increasing inelastic phonon interface scattering tends to increase the phonon transmission coefficients and decrease the thermal boundary resistance was provided by Swartz and Pohl.[1] Here, we adapt their explanation for our discussion of the Si/Ge interface. If a phonon incident on the Si/Ge interface from the Si side has a frequency greater than the maximum Ge frequency, none of its energy can transmit across the interface if the phonon can only scatter elastically. On the other hand, there is a possibility for energy transmission if the phonon can scatter inelastically into two phonons of lower frequency. Inelastic phonon scattering thus increases the available channels for thermal conductance across the interface and decreases the thermal boundary resistance. We note that similar trends of decreasing thermal boundary resistance with increasing temperature have been predicted from MD[22] and observed experimentally,[9,14,15] and attributed to inelastic phonon interface scattering.

In Fig. 6, we show the MD predictions of the thermal boundary resistance for the Si/heavy-Si interfaces as a function of mass ratio at a temperature of 500 K. The 95% confidence interval is provided for two of the data points. The thermal boundary resistance decreases monotonically with decreasing mass ratio and approaches zero for $m_R=1$, the case where no interface is present in the system. We expect that the phonons scatter elastically at all the Si/heavy-Si interfaces at this temperature. This expectation is based on (i)

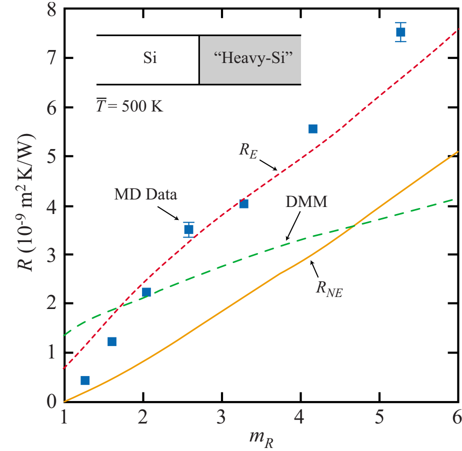

FIG. 6. (Color online) Thermal boundary resistance of the Si/heavy-Si interface plotted as a function of mass ratio (m_R) at a temperature of 500 K. The lines labeled R_E and R_{NE} correspond to the results of theoretical calculations assuming that the phonons scatter elastically and specularly at the interface and have either equilibrium or bulk-like nonequilibrium distributions (see Sec. II B). The line labeled DMM corresponds to the theoretical calculations of the diffuse mismatch model, which assumes that the phonons scatter elastically and diffusely at the interface and have equilibrium distributions.

the fact that a heavy-Si atom samples a more harmonic potential well than a Si atom because of its smaller mean-square atomic displacement,[54] and (ii) the observation that the anharmonicity in Si does not lead to significant inelastic scattering at the Si/Ge interface at this temperature (see Fig. 5).

B. Comparison with theoretical predictions

We assess the accuracy of the theoretical expressions for the thermal boundary resistance by comparing their predictions to the MD-predicted values. For the Si/Ge interface, we calculate R_E [Eq. (9)] to be 3.0×10^{-9} m^2-K/W in the classical limit. As shown in Fig. 5, this value is in good agreement with the MD predictions at and below a temperature of 500 K, where the phonon scattering is predominantly elastic. Our value of R_E is also within 5% of the value of 2.85 $\times10^{-9}$ m^2-K/W calculated by Zhao and Freund for the SW Si/Ge interface using a similar LD-based method, and extrapolated by us to the classical limit.[37] The small difference between the calculations is due to lattice mismatch strain, which was neglected by Zhao and Freund. For the Si/heavy-Si interfaces at a temperature of 500 K (Fig. 6), R_E is in agreement with the MD-predicted values to within 12% for $m_R\geq2$. As expected, R_E is erroneously nonzero when no interface is present in the system (i.e., $m_R=1$).

Our calculations for R_{NE} [Eq. (10)], which are also provided in Figs. 5 and 6, are in poor agreement with the MD-predicted thermal boundary resistances. For the Si/Ge interface in the classical limit, we find that R_{NE} is 1.3 $\times10^{-9}$ m^2-K/W, approximately 60% less than the MD-predicted values in the low temperature, elastic scattering regime. For the Si/heavy-Si interfaces at a temperature of

500 K, R_{NE} decreases with decreasing mass ratio and is equal to zero when no interface is present in the system, consistent with the MD-predicted trend. Over the entire mass ratio range, however, R_{NE} is 40%–60% less than the MD-predicted values.

Our observations are consistent with the findings of Aubry *et al.*[24] and Kimmer *et al.*,[23] who compared MD-predicted thermal resistances to theoretically calculated values for two SW Si grain boundaries at a temperature of 500 K. They used input from MD wave-packet simulations and assumed that either τ or the product τv_z was constant for all modes in their theoretical calculations. They predict the thermal resistance of the $\Sigma3(111)$ grain boundary from MD to be 0.1×10^{-9} m^2-K/W, a value within 20%–60% of R_{NE} and a factor of 8 less than R_E. Based on the MD-predicted thermal resistance, we believe that the level of phonon scattering at this grain boundary is similar to that at a Si/heavy-Si interface with m_R=1.1. For this interface, we would expect to obtain a similar relationship between R_E, R_{NE} and the MD-predicted thermal boundary resistance based on the trends shown in Fig. 6. For the $\Sigma29(001)$ grain boundary, their MD-predicted thermal resistance is 1.3×10^{-9} m^2-K/W, a value within 10% of R_E but 50% greater than R_{NE}. Based on the MD-predicted thermal resistance, we believe that the level of phonon scattering at this grain boundary is comparable to that for a Si/heavy-Si interface with m_R=1.6, for which R_E is also in closer agreement with the MD-predicted thermal boundary resistance than R_{NE}.

As mentioned in Sec. II C, we evaluate R_E and R_{NE} by assuming that the phonon interface scattering is specular and elastic. Both assumptions must be valid in the MD simulations to provide an accurate assessment of the theoretical expressions for the thermal boundary resistance. We have already demonstrated for our interfaces that the assumption of elastic scattering is valid at temperatures less than or equal to ~500 K (see Sec. IV A). Because our interfaces contain no defects or roughness that would promote diffuse scattering, we also expect that the assumption of specular scattering is valid. For additional evidence of this claim we compare the MD-predicted thermal boundary resistances to values calculated using Eq. (9) with the phonon transmission coefficients determined by the DMM,[1,19] where all phonons are assumed to scatter diffusely at the interface. In these calculations, all of the phonon properties required to evaluate the DMM-phonon transmission coefficients are obtained from harmonic LD-based calculations. As shown in Fig. 5, we find that the DMM-predicted thermal boundary resistance for the Si/Ge interface is 20% less than the MD-predicted values in the low temperature, elastic scattering regime. This agreement is believed to be fortuitous, however, because for the Si/heavy-Si interfaces (see Fig. 6), the DMM- and MD-predicted thermal boundary resistances are in poor agreement at all mass ratios except near $m_R \approx 2$, which is close to the atomic mass ratio between Ge and Si of 2.6. Because R_E is in better agreement with the MD-predicted thermal boundary resistances than the DMM-predicted values, we believe that the assumption of specular phonon scattering is valid for our interfaces.

Even when the phonon interface scattering is specular and elastic, neither R_E nor R_{NE} is in good agreement with the MD-predicted thermal boundary resistances for all of the interfaces examined here. For R_E, the inaccuracy observed for the Si/heavy-Si interfaces with $m_R < 2$ is due to the assumption of equilibrium phonon distributions in each lead, as mentioned in Sec. II B 1. For R_{NE}, we attribute the observed inaccuracy to our assumption of bulk-like nonequilibrium phonon distributions near the interface. According to the BTE, the steady-state phonon distribution for a given mode at position $\mathbf{r}$ is such that the rate of phonon creation and annihilation is balanced by the rate that phonons leave the neighborhood of $\mathbf{r}$ due to diffusion.[10,11] In a bulk crystal with no defects, the phonon creation and annihilation rates are determined by inelastic multi-phonon scattering processes, which are accounted for in the anharmonic LD-based calculations described in Sec. II C 1. Near an interface, however, the phonon creation and annihilation rates will be affected by phonon scattering at the interface, leading to phonon distributions that are different from those in the bulk. Because R_E is in good agreement with the MD predictions for the Si/Ge interface and the Si/heavy-Si interfaces with $m_R > 2$, we hypothesize that for these interfaces these additional scattering processes lead to phonon distributions that are well approximated by the equilibrium distribution at T_L or T_R. To test this hypothesis, we believe that a more accurate prediction for the phonon distributions near the interface can be obtained by solving the BTE while incorporating the interface scattering processes into the collision term. We suspect that such a solution procedure may be complicated by the potential inaccuracy of the relaxation time approximation near the interface. Under this approximation, only the phonon mode of interest is assumed to be out of equilibrium,[10] which is reasonable for systems that are not far from equilibrium[51] but questionable near the interface due to the abrupt temperature drop. If such inaccuracy exists, a variational approach will be required to solve the BTE.[10]

V. SUMMARY AND CONCLUSIONS

We assessed the accuracy of two theoretical expressions for thermal boundary resistance by comparing their predictions to independent predictions from MD simulations, which require no assumptions concerning the nature of the phonon scattering. The theoretical expressions differ in their assumed form of the phonon distribution functions in the leads on either side of the interface (see Fig. 1). In one expression (R_E), the phonon distributions are assumed to follow the equilibrium, Bose-Einstein distribution, while in the other expression (R_{NE}), the phonons are assumed to have nonequilibrium distributions. We obtained the nonequilibrium phonon distributions by solving the BTE under the relaxation time approximation and under the assumption that the phonon distributions in each lead near the interface are bulk like. The phonon properties required to evaluate the theoretical expressions were obtained using LD-based methods. For the calculation of the phonon transmission coefficients, we used the LD-based scattering boundary method, which assumes that the phonon interface scattering is elastic and specular. To allow a proper comparison to the predictions from the classical MD simulations, the theoretical ex-

pressions were evaluated in the classical limit.

The theoretically calculated and MD-predicted thermal boundary resistances were compared for (i) a symmetrically-strained Si/Ge interface between temperatures of 300 and 1000 K, and (ii) a series of Si/heavy-Si interfaces at a temperature of 500 K. All of the interfaces are perfect and contain no defects or roughness that would promote diffuse interface scattering, justifying the assumption of specular interface scattering made in our calculations of the phonon transmission coefficients.

As shown in Fig. 5, the Si/Ge thermal boundary resistance was predicted from MD to decrease with increasing temperature for temperatures above ~500 K, a trend indicative of phonon interface scattering that is inelastic. At temperatures less than or equal to ~500 K, the Si/Ge MD-predicted thermal boundary resistance was found to be temperature independent, indicating that the phonon interface scattering is predominately elastic. For the Si/heavy-Si interfaces at a temperature of 500 K (see Fig. 6), the MD-predicted thermal boundary resistance decreases with decreasing mass ratio and approaches a value of zero for $m_R=1$ (i.e., an imaginary Si/Si interface). We argued that the phonon interface scattering is elastic at the Si/heavy-Si interfaces at a temperature of 500 K. This argument was based on the MD-predicted temperature dependence for the Si/Ge thermal boundary resistance and the mass dependence of the mean-square atomic displacement.

With the exception of the Si/heavy-Si interfaces with $m_R < 2$, the theoretical calculations of R_E were found to be in good agreement with the MD-predicted thermal boundary resistances at temperatures where the phonon scattering is elastic. The inaccuracy of R_E observed for the Si/heavy-Si interfaces with $m_R<2$ is most extreme at $m_R=1$ where R_E is erroneously nonzero. This inaccuracy has been attributed to the assumption of equilibrium phonon distributions in each lead.[6,49] The theoretical expression for R_{NE} gives the correct result of zero thermal boundary resistance for the Si/heavy-Si interface with $m_R=1$. For the Si/Ge interface and for the Si/heavy-Si interfaces with $m_R>1$, however, R_{NE} was found to be 40%–60% less than the corresponding MD-predicted thermal boundary resistances at temperatures where the phonon interface scattering is elastic. We attributed this inaccuracy to our assumption of bulk-like phonon distributions in each lead. The phonon distributions near the interface will deviate from their bulk values due to the additional phonon creation and annihilation processes that are associated with the phonon interface scattering. We suggest that the accuracy of the R_{NE} calculations can be improved if the phonon distributions in each lead near the interface are obtained by solving the BTE while incorporating these additional processes into the collision term.

ACKNOWLEDGMENTS

We thank J. E. Turney (CMU) for providing the phonon relaxation times and T. Matsuura (CMU) for contributing to the methodology of the MD predictions.

*mcgaughey@cmu.edu

[1] E. T. Swartz and R. O. Pohl, Rev. Mod. Phys. **61**, 605 (1989).
[2] D. Roberts and G. Triplett, Solid-State Electron. **52**, 1669 (2008).
[3] Y. L. Li, Y. R. Huang, and Y. H. Lai, Appl. Phys. Lett. **91**, 181113 (2007).
[4] G. Chen, M. S. Dresselhaus, G. Dresselhaus, J.-P. Fleurial, and T. Caillat, Int. Mater. Rev. **48**, 45 (2003).
[5] M. S. Dresselhaus, G. Chen, M. Y. Tang, R. G. Yang, H. Lee, D. Z. Wang, Z. F. Ren, J. Fleurial, and P. Gogna, Adv. Mater. **19**, 1043 (2007).
[6] W. A. Little, Can. J. Phys. **37**, 334 (1959).
[7] R. J. Stoner and H. J. Maris, Phys. Rev. B **48**, 16373 (1993).
[8] A. Majumdar and P. Reddy, Appl. Phys. Lett. **84**, 4768 (2004).
[9] H. K. Lyeo and D. G. Cahill, Phys. Rev. B **73**, 144301 (2006).
[10] G. P. Srivastava, *The Physics of Phonons* (Adam Hilger, Bristol, 1990).
[11] J. M. Ziman, *Electrons and Phonons* (Oxford University Press, New York, 2001).
[12] T. Beechem, S. Graham, P. Hopkins, and P. Norris, Appl. Phys. Lett. **90**, 054104 (2007).
[13] P. E. Hopkins, P. M. Norris, R. J. Stevens, T. E. Beechem, and S. Graham, ASME J. Heat Transfer **130**, 062402 (2008).
[14] P. E. Hopkins, P. M. Norris, and R. J. Stevens, ASME J. Heat Transfer **130**, 022401 (2008).
[15] P. E. Hopkins and P. M. Norris, ASME J. Heat Transfer **131**, 022402 (2009).
[16] R. S. Prasher and P. E. Phelan, ASME J. Heat Transfer **123**, 105 (2001).
[17] R. M. Costescu, M. A. Wall, and D. G. Cahill, Phys. Rev. B **67**, 054302 (2003).
[18] R. J. Stevens, A. N. Smith, and P. M. Norris, ASME J. Heat Transfer **127**, 315 (2005).
[19] P. Reddy, K. Castelino, and A. Majumdar, Appl. Phys. Lett. **87**, 211908 (2005).
[20] N. S. Snyder, Cryogenics **10**, 89 (1970).
[21] R. J. Stoner, H. J. Maris, T. R. Anthony, and W. F. Banholzer, Phys. Rev. Lett. **68**, 1563 (1992).
[22] R. J. Stevens, L. V. Zhigilei, and P. M. Norris, Int. J. Heat Mass Tranfer **50**, 3977 (2007).
[23] C. Kimmer, S. Aubry, A. Skye, and P. K. Schelling, Phys. Rev. B **75**, 144105 (2007).
[24] S. Aubry, C. J. Kimmer, A. Skye, and P. K. Schelling, Phys. Rev. B **78**, 064112 (2008).
[25] S. Choi and S. Maruyama, Int. J. Therm. Sci. **44**, 547 (2005).
[26] C. J. Twu and J. R. Ho, Phys. Rev. B **67**, 205422 (2003).
[27] A. J. H. McGaughey, M. I. Hussein, E. S. Landry, M. Kaviany, and G. M. Hulbert, Phys. Rev. B **74**, 104304 (2006).
[28] B. C. Daly, H. J. Maris, K. Imamura, and S. Tamura, Phys. Rev. B **66**, 024301 (2002).
[29] E. S. Landry, M. I. Hussein, and A. J. H. McGaughey, Phys. Rev. B **77**, 184302 (2008).

[30] E. S. Landry and A. J. H. McGaughey, Phys. Rev. B **79**, 075316 (2009).
[31] Y. Chen, D. Li, J. R. Lukes, Z. Ni, and M. Chen, Phys. Rev. B **72**, 174302 (2005).
[32] S. Volz, J. B. Saulnier, G. Chen, and P. Beauchamp, Microelectron. J. **31**, 815 (2000).
[33] P. K. Schelling, S. R. Phillpot, and P. Keblinski, Appl. Phys. Lett. **80**, 2484 (2002).
[34] A. J. H. McGaughey and M. Kaviany, Phys. Rev. B **69**, 094303 (2004).
[35] J. Shiomi and S. Maruyama, Int. J. Thermophys. (2008).
[36] D. A. Young and H. J. Maris, Phys. Rev. B **40**, 3685 (1989).
[37] H. Zhao and J. B. Freund, J. Appl. Phys. **97**, 024903 (2005).
[38] J. Wang and J. Wang, J. Phys.: Condens. Matter **19**, 236211 (2007).
[39] W. Zhang, T. S. Fisher, and N. Mingo, ASME J. Heat Transfer **129**, 483 (2007).
[40] J. Wang, J. Wang, and J. T. Lu, Eur. Phys. J. B **62**, 381 (2008).
[41] N. Mingo, Phys. Rev. B **74**, 125402 (2006).
[42] F. H. Stillinger and T. A. Weber, Phys. Rev. B **31**, 5262 (1985).
[43] K. Ding and H. C. Andersen, Phys. Rev. B **34**, 6987 (1986).
[44] M. Laradji, D. P. Landau, and B. Dunweg, Phys. Rev. B **51**, 4894 (1995).
[45] L. G. C. Rego and G. Kirczenow, Phys. Rev. Lett. **81**, 232 (1998).
[46] N. Mingo and D. A. Broido, Phys. Rev. Lett. **95**, 096105 (2005).
[47] G. Chen, Phys. Rev. B **57**, 14958 (1998).
[48] S. Pettersson and G. D. Mahan, Phys. Rev. B **42**, 7386 (1990).
[49] S. Simons, J. Phys. C **7**, 4048 (1974).
[50] G. Chen, Appl. Phys. Lett. **82**, 991 (2003).
[51] J. E. Turney, A. J. H. McGaughey, and C. H. Amon, Phys. Rev. B **79**, 224305 (2009).
[52] J. Wang and J. S. Wang, Phys. Rev. B **74**, 054303 (2006).
[53] E. S. Landry, Ph.D. thesis, Carnegie Mellon University.
[54] M. T. Dove, *Introduction to Lattice Dynamics* (Cambridge University Press, Cambridge, England, 1993).
[55] J. Callaway, Phys. Rev. **113**, 1046 (1959).
[56] J. E. Turney, E. S. Landry, A. J. H. McGaughey, and C. H. Amon, Phys. Rev. B **79**, 064301 (2009).
[57] G. Theodorou, in *Properties of Silicon Germanium and SiGe:Carbon*, edited by E. Kasper and K. Lyutovich (INSPEC, The Institution of Electrical Engineers, London, 2000), pp. 91–93.
[58] E. R. Cowley, Phys. Rev. Lett. **60**, 2379 (1988).
[59] T. Ikeshoji and B. Hafskjold, Mol. Phys. **81**, 251 (1994).
[60] N. W. Ashcroft and N. D. Mermin, *Solid State Physics* (Sauders College Publishing, Fort Worth, 1976).
[61] T. Borca-Tasciuc *et al.*, Superlattices Microstruct. **28**, 199 (2000).
[62] Our estimate of the experimental Si/Ge thermal boundary resistance can only be considered accurate to an order of magnitude for two reasons. First, the interfaces are not isolated from each other, as they are separated by a distance much less than the bulk phonon mean free paths [e.g., the average phonon mean free path in Si is estimated to be 300 nm at room temperature (Ref. 63)]. Second, the lattice mismatch between Si and Ge will lead to strain-induced defects (e.g., misfit dislocations) at a realistic Si/Ge interface (Refs. 30 and 57).
[63] Y. S. Ju and K. E. Goodson, Appl. Phys. Lett. **74**, 3005 (1999).
[64] www.gnu.org/software/gsl/